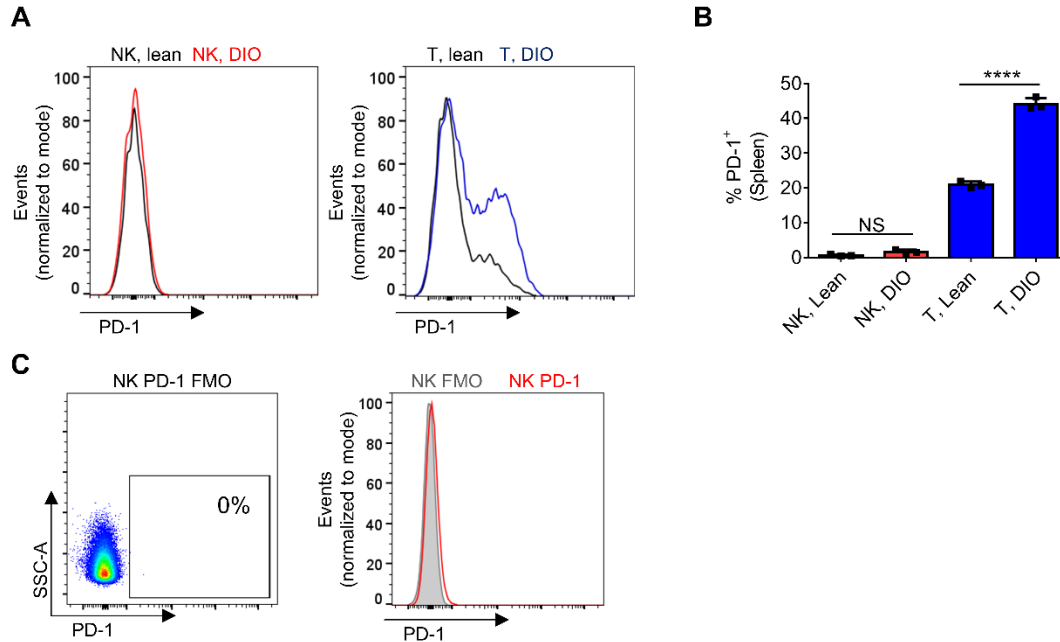
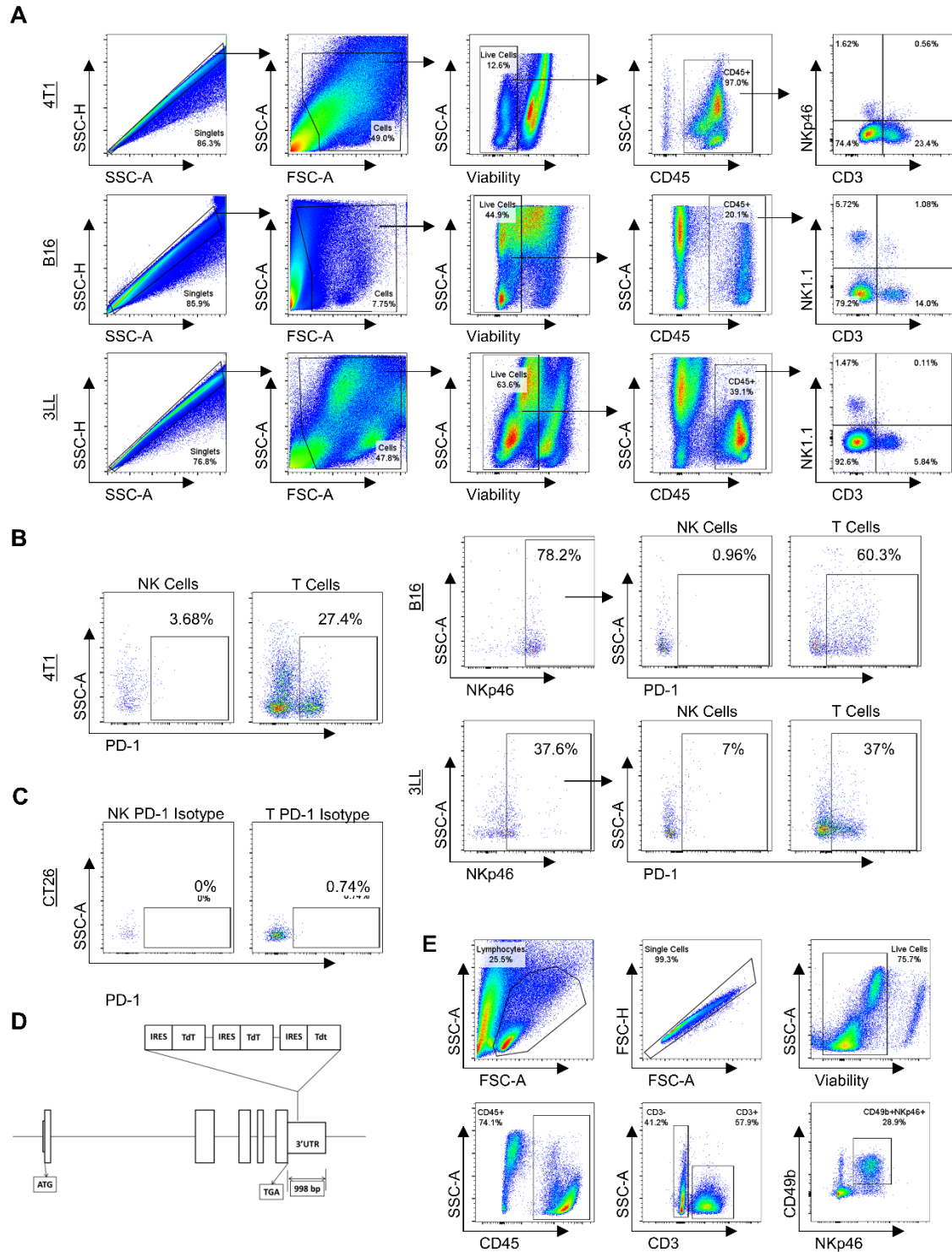


Supplemental Figure 1. Gating strategy for identification of mouse NK and T cells *in vitro*. Gating strategy for analysis of NK and T cells from cytokine-activated mouse splenocytes, gating of singlets, cells, live cells, NK1.1 vs CD3.

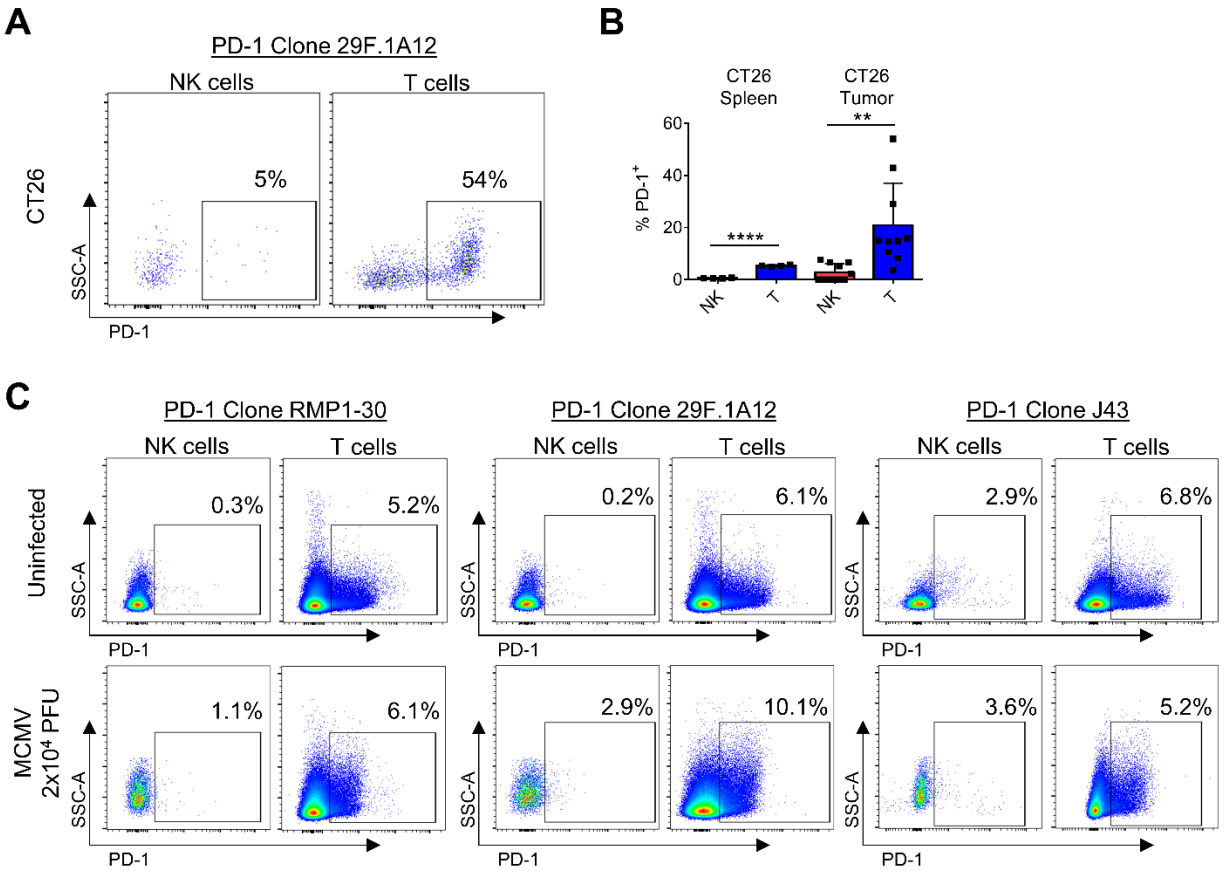


Supplemental Figure 2. Diet-induced obesity does not lead to upregulation of NK PD-1. (A) Representative histogram showing PD-1 staining intensity on NK cells and T cells isolated from the spleens of lean and DIO mice, and (B) summary data for PD-1 expression. T cells from DIO mice show increased PD-1 expression, while NK cell expression of PD-1 remained minimal in both groups. (C) Dot plot of PD-1 FMO and histogram of PD-1 FMO and NK full stain. Mean \pm SD for $n = 3$ donors/group. **** $P < 0.0001$, unpaired Student's t-test. NS, not significant. FMO, fluorescence minus one.

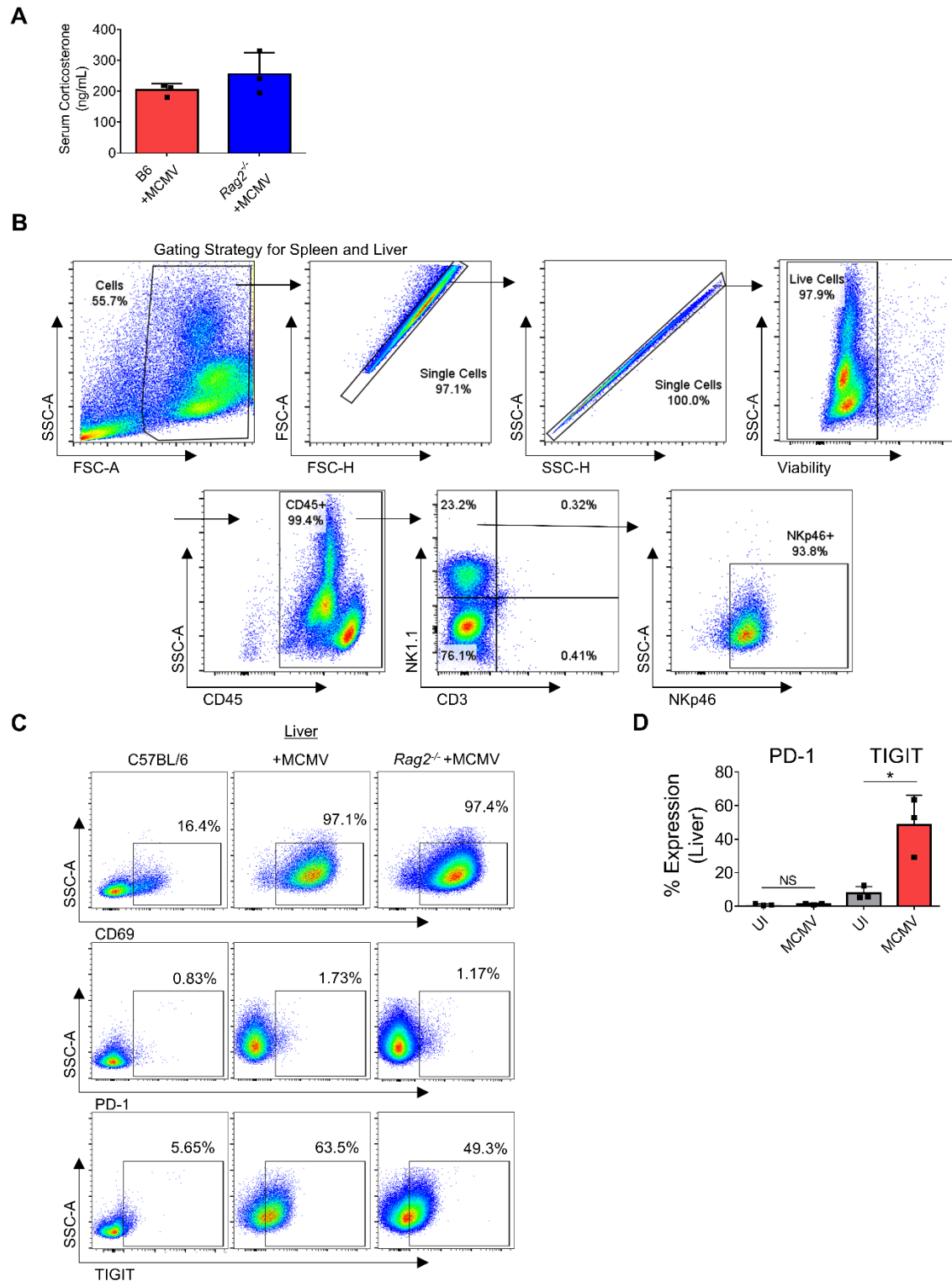


Supplemental Figure 3. Gating strategy and identification of NK and T cells from tumor models. (A) Gating strategy for analysis of intra-tumoral NK and T cells generated by subcutaneous implantation of 4T1, B16, and 3LL tumors in BALB/c or

C57BL/6 mice. NK cells further gated on NKp46⁺ in C57BL/6 mice. **(B)** Representative NK and T cell parent gating on 4T1, B16, and 3LL intra-tumoral lymphocytes in addition to PD-1 expression on NK and T cells. **(C)** Representative flow cytometry showing PD-1 expression on NK and T cells compared to isotype control in CT26 tumor. **(D)** Schematic genetic map showing the design of the PD-1 reporter mouse and TdTomato fluorescent protein insertion. **(E)** Representative gating strategy for analysis of NK and T cells within the CT26 tumor from PD-1 reporter mice.

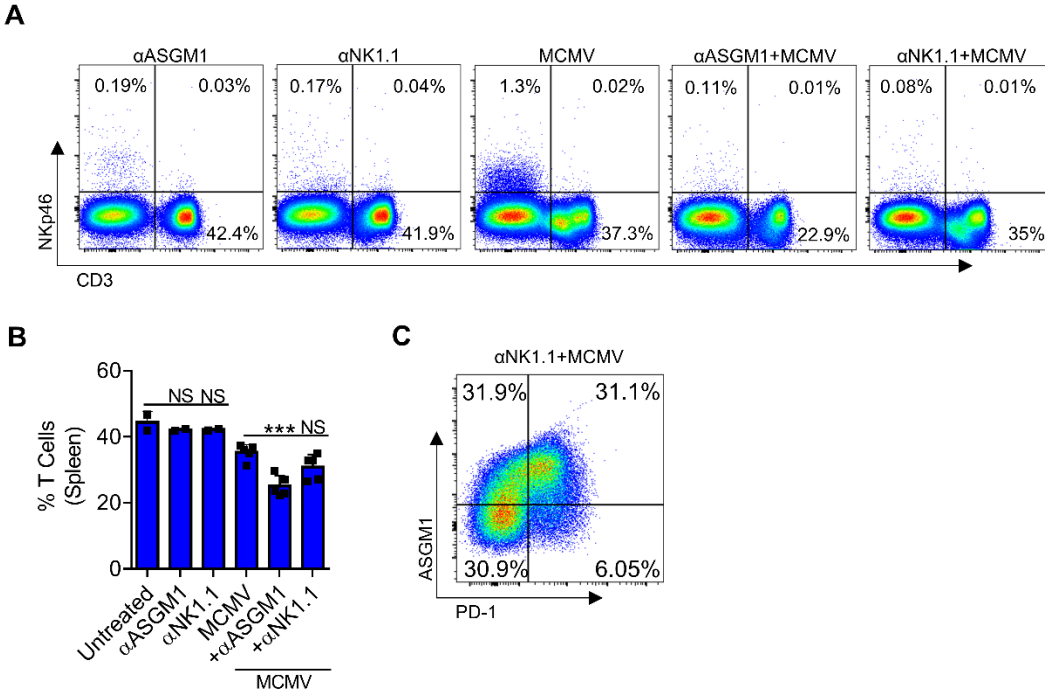


Supplemental Figure 4. In vivo detection of PD-1 using additional anti-PD-1 antibodies. (A) Representative PD-1 staining on intra-tumoral NK and T cells from subcutaneous CT26 tumors. (B) Quantitative data showing PD-1 expression on splenic and intra-tumoral NK and T cells from CT26-bearing mice with PD-1 expression significantly higher on splenic and intra-tumoral T cells compared to NK cells. (C) Representative PD-1 staining using three anti-PD-1 clones on splenic NK and T cells in uninfected and MCMV-infected mice 3 days post-infection. Mean \pm SD, for n = 4-10 mice/group. ** $P < 0.01$, **** $P < 0.0001$, paired Student's t-test.

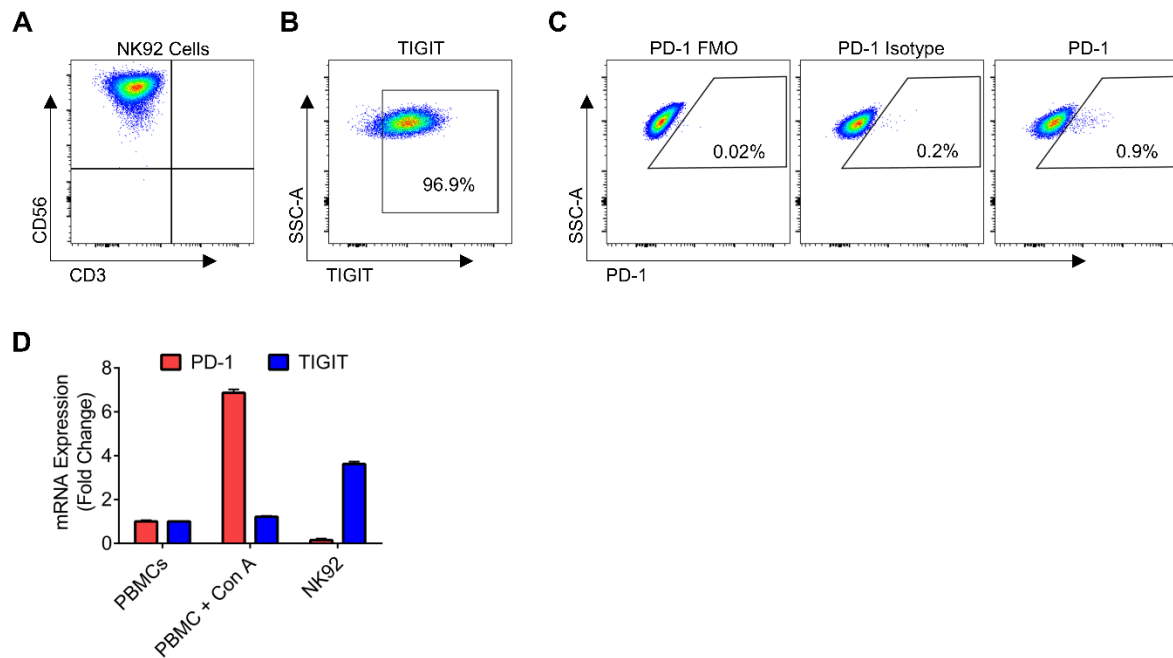


Supplemental Figure 5. Gating strategy and liver NK cell expression following acute MCMV. (A) Similar corticosterone levels were measured in the serum of MCMV-

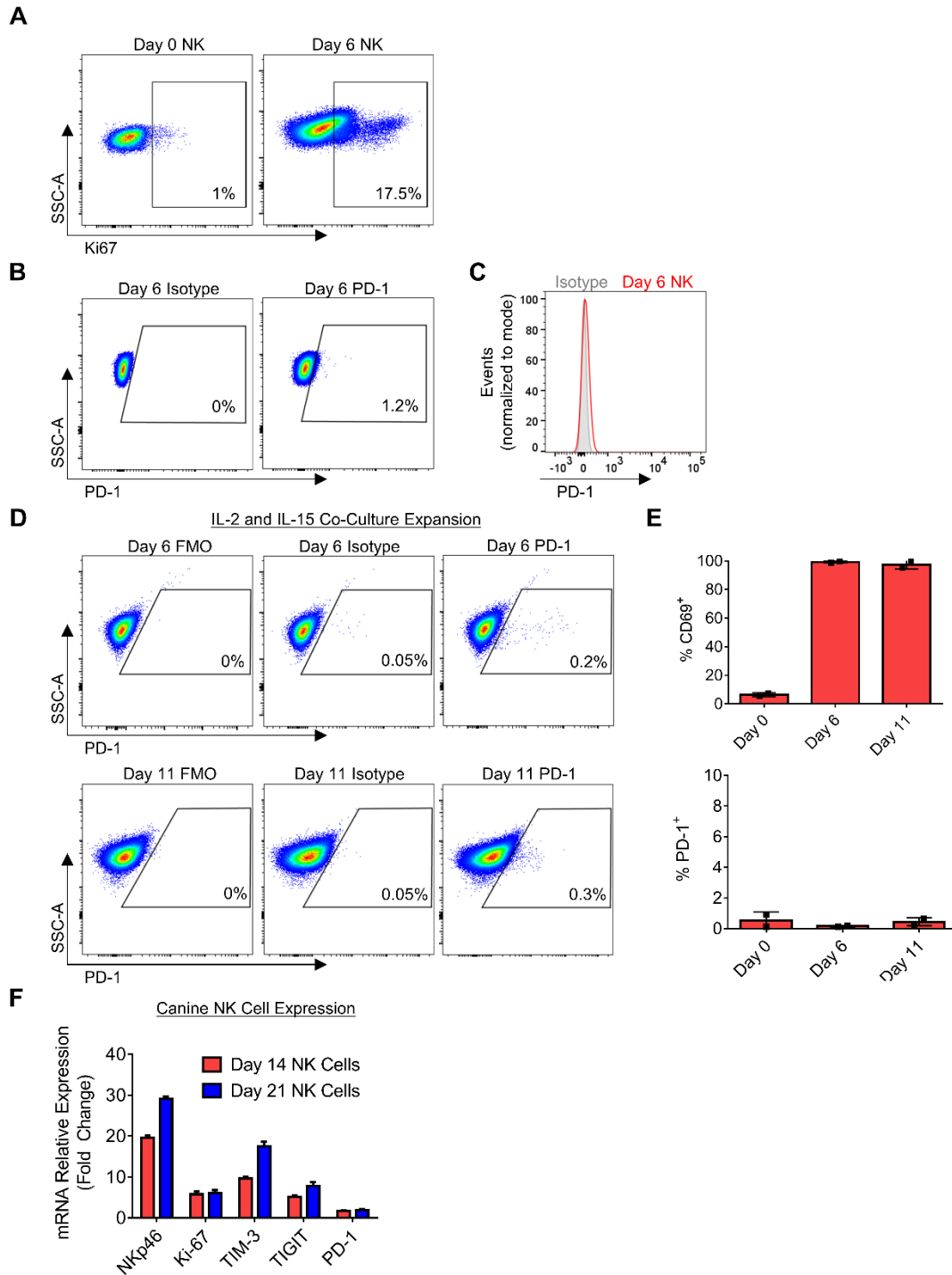
infected WT and *Rag2*^{-/-} mice at 48 h post-infection. **(B)** Representative gating strategy from *Rag2*^{-/-} spleen that was used for analysis of NK and T cells in both spleen and liver of all mice evaluated. **(C)** Representative flow cytometry and **(D)** summary data showing increase in activation marker CD69 expression with MCMV infection, and no significant PD-1 expression on NK cells. Percent TIGIT expression increases significantly on liver NK cells with acute MCMV infection. Mean \pm SD for n = 3 mice/group and representative of 3 independent experiments. **P* < 0.05, unpaired Student's t-test **(D)**. UI, uninfected.



Supplemental Figure 6. NK and T cell changes with anti-ASGM1 versus anti-NK1.1 with acute MCMV infection. (A) Parent gating showing NK and T cell populations in all treatment groups. NK cells are depleted with ASGM1 and NK1.1 targeting, while T cells are depleted in ASGM1 depletion with MCMV infection only. **(B)** Percent T cells in each treatment group compared to untreated or MCMV infection only group. **(C)** ASGM1⁺PD-1⁺ proportion remains present in group with MCMV infection and NK1.1 depletion. Mean \pm SD for n = 2-5 mice/group and representative of 2 independent experiments. *** $P < 0.001$, one-way ANOVA. NS, not significant.

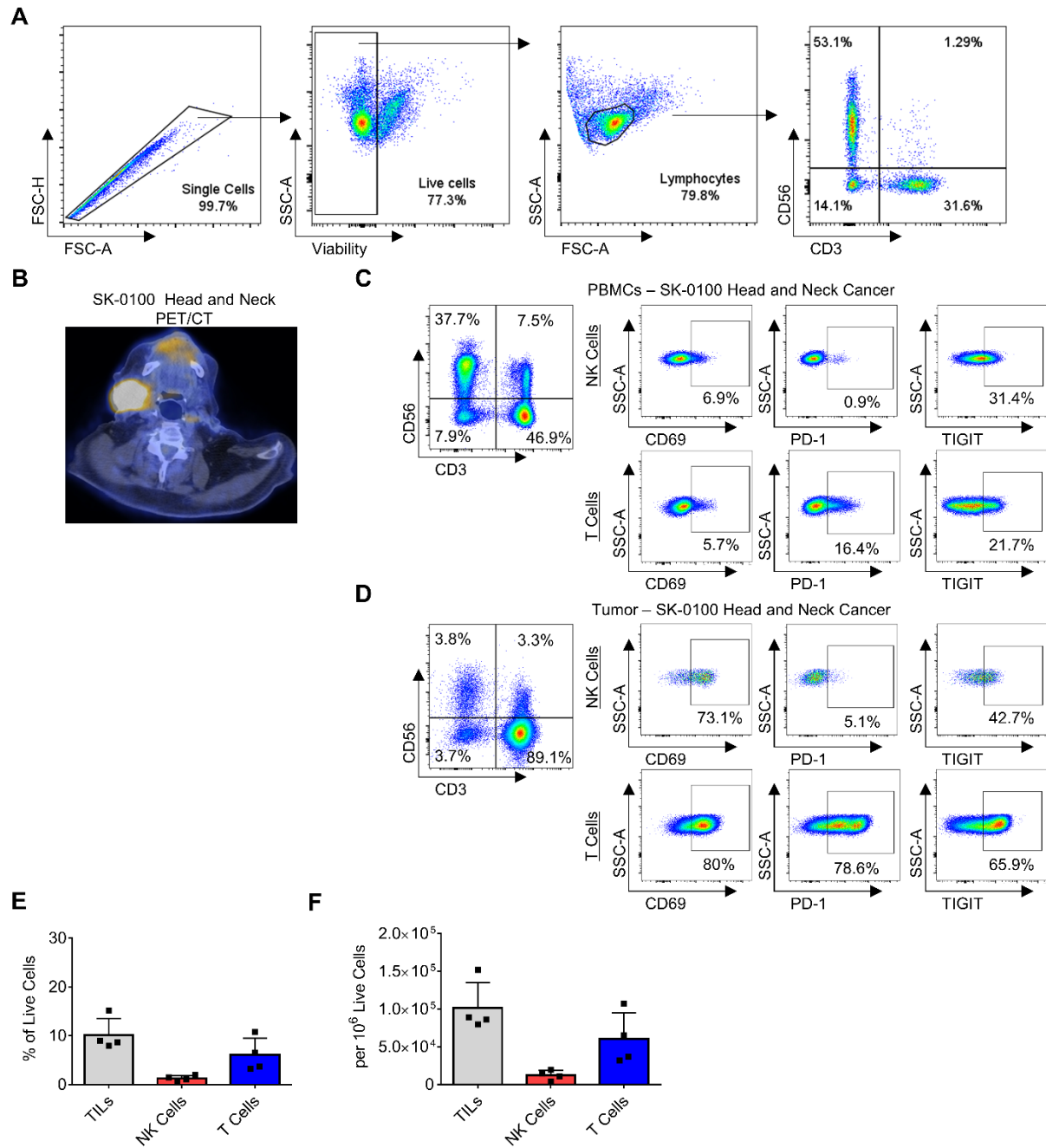


Supplemental Figure 7. Minimal PD-1 expression by NK92 cells. (A) Representative gating for analysis of NK92 cells after in vitro culture in 500 IU/mL rhIL-2. Cells are CD3⁻CD56^{bright} and (B) highly express TIGIT, (C) but lack expression of PD-1 as seen by gating comparing FMO, isotype, and PD-1 stain. (D) qRT-PCR analysis of NK92 cells confirms minimal expression of PD-1 and increased expression of TIGIT as compared to resting, healthy human PBMCs. ConA stimulated PBMCs shown for positive control for PD-1 detection. FMO, fluorescence minus one. ConA, concanavalin A.



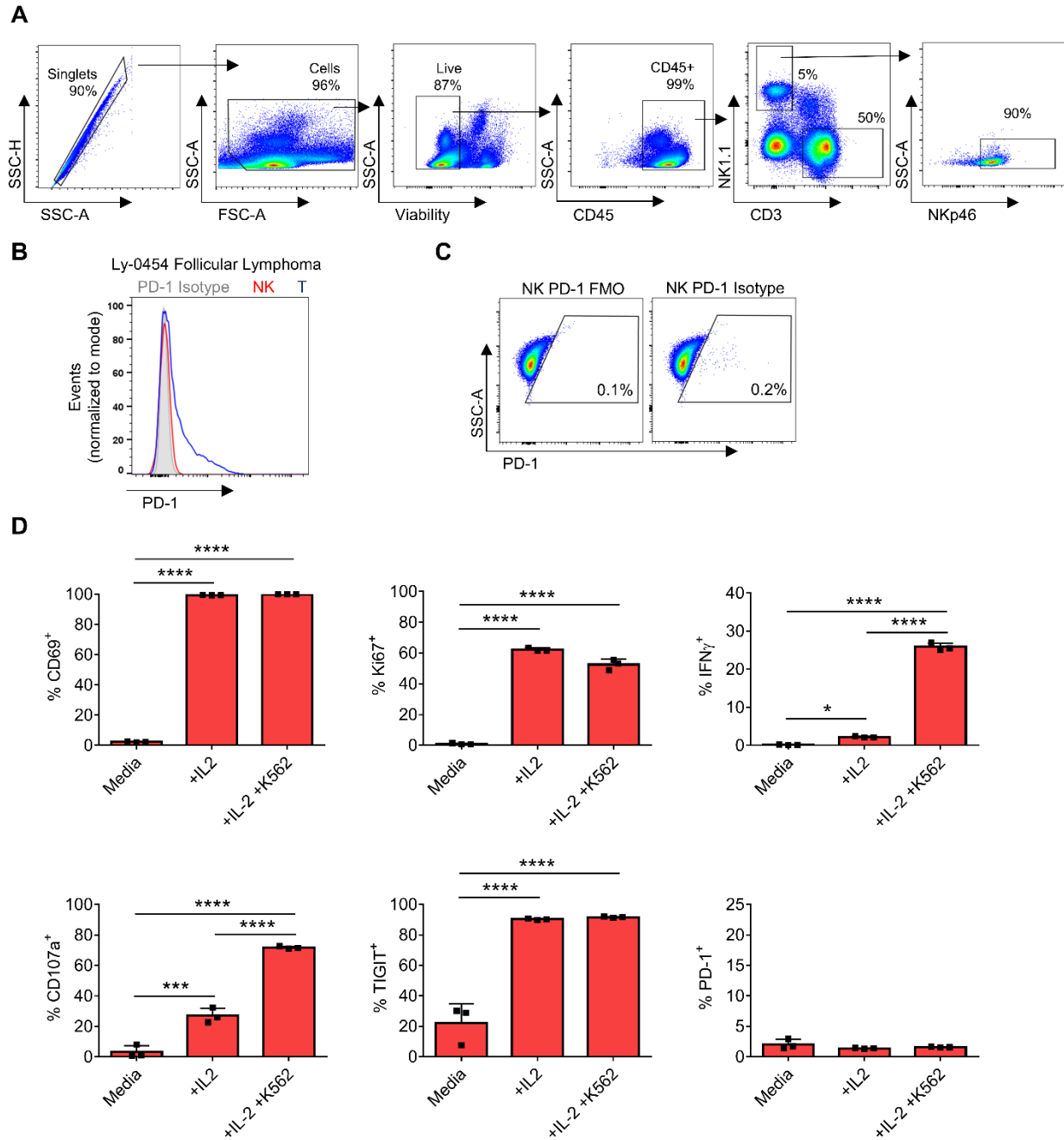
Supplemental Figure 8. Minimal PD-1 expression by ex vivo activated NK cells in IL-2 and/or IL-15 co-culture. (A) Representative flow cytometry for Ki67 expression at day 0 and day 6 showing the increase in expression of proliferation marker Ki67. **(B)**

Representative gating from day 6 co-culture expansion showing PD-1 isotype and PD-1 stain on NK cells, **(C)** and representative histogram of staining intensity compared to isotype control. **(D)** PD-1 FMO, isotype, and full stain on NK cells expanded using the co-culture feeder line (K562.C19) supplemented with rhIL-2 and rhIL-15. **(E)** Summary data showing CD69 and PD-1 expression from two unique healthy donors at days 0, 6 and 11 of co-culture expansion. **(F)** qRT-PCR analysis of expanded canine NK cells showing increased expression of NKp46, Ki67, TIM-3, and TIGIT, with minimal expression of PD-1 at day 14 and 21, as compared to freshly isolated canine NK cells. Means \pm SD for n = 2 individual human donors. **(D)** Canine data from single NK expansion. Representative of 3-4 **(A-C)** or 2 **(D-F)** independent experiments. FMO, fluorescence minus one.



Supplemental Figure 9. Gating strategy for human tumor samples and analysis of head and neck cancer. (A) Representative gating strategy for analysis of peripheral and intra-tumoral NK and T cells from human cancer patients (colon cancer tumor shown). **(B)** Pre-operative PET/CT imaging showing hypermetabolic tumor in head and neck cancer patient. **(C)** Parent gating showing NK and T cell populations and NK and T

cell phenotype from the peripheral blood and **(D)** intra-tumoral microenvironment of a patient with head and neck squamous cell carcinoma. **(E)** Percent of live cells, and **(F)** total cells represented by TILs, NK cells and T cells among all sarcomas analyzed. Within sarcomas (n = 4), NK cells represent a paucity of immune cells present.



Supplemental Figure 10. Gating strategy for human lymphoma and phenotype of cytotoxic human NK cells in vitro. (A) Representative gating strategy for analysis of peripheral and intra-tumoral NK and T cells from follicular lymphoma patient (peripheral blood shown). (B) Histogram of PD-1 expression on intra-tumoral NK and T cells compared to isotype control. (C) Dot plots showing PD-1 FMO and isotype controls from

cytotoxic NK cells cultured with rhIL-2 and K562 target cells. (D) Expression of activation and functional markers compared between media only, rhIL-2-activated NK cells, and NK cells cultured with rhIL-2 and K562 target cells. Mean \pm SD, with $n=3$ /group, representative of 2 independent experiments. *** $P < 0.001$, **** $P < 0.0001$, one-way ANOVA with multiple group comparisons.

Supplemental Table 1. Species-specific primers for qRT-PCR analysis

Species	Gene Name	Forward 5'	Reverse 5'
Human	<i>MKI67</i>	TAACGCGGAGTGCAAGAGG	TCACTGTCCCTATGACTTCTGG
Human	<i>PDCD1</i>	CCCTGGTGGTTGGTGTCG	CCCCATAGTCCACAGAGAACAC
Human	<i>TIGIT</i>	BioRad	BioRad
Human	<i>B2M</i>	GAGTATGCCTGCCGTGTGAA	TGCGGCATCTTCAAACCTCC
Human	<i>IPO8</i>	TTATGCTTCTCCCACCACAGC	AGGGTCAAAGTTCGGGTCTG
Mouse	<i>Pdcd1</i>	Qiagen	Qiagen
Mouse	<i>Gzmb</i>	GCTGCTAAAGCTGAAGAGTAAG	CCAGCCACATAGCACACATC
Mouse	<i>Gapdh</i>	Qiagen	Qiagen
Canine	<i>NCR1</i>	BioRad	BioRad
Canine	<i>MKI67</i>	BioRad	BioRad
Canine	<i>HAVCR2</i>	BioRad	BioRad
Canine	<i>TIGIT</i>	BioRad	BioRad
Canine	<i>PDCD1</i>	BioRad	BioRad
Canine	<i>GAPDH</i>	TGTCCCCACCCCAATGTATC	CTCCGATGCCTGCTTCACTACCTT

Supplemental Methods

PD-1 TdTomato Reporter Mice. To generate the IRES/TdTomato reporter mouse, an 8573bp fragment of the PD-1 locus (from 5000bp upstream and 3570bp downstream of stop codon) was sub-cloned from a C57BL/6J BAC clone (RP23 16F24) into vector pKO LSLR. A 1431bp coding sequence for Tdtomato was introduced downstream of 566bp IRES sequence, and this 1997bp reporter was multimerized three times to generate three tandem repeats of IRES/Tdtomato. This 3x reporter was inserted 130bp downstream of the stop codon in the 3'UTR region. A Neo cassette, flanked with FRT sites, was introduced between the reporter and 3'homology arm. B6 ES cells (Primogenix, Inc., St. Louis, MO) were electroporated with 20 micrograms of linearized targeting vector and single colonies were isolated under positive (Neo) and negative (DTA –from vector backbone) selection. Ninety-six colonies were screened with a long-range PCR to give 10 positive clones. Five clones were grown for further validation, and Southern analyses with 5' and 3' probes showed that 2/5 clones had all 3 copies of the IRES/Tdtomato reporter while 3/5 clones had only 2 copies of the reporter. The 2 clones showing all 3 copies of the reporter were injected into blastocysts to generate chimeras, which were mated to FLPE-expressing line to generate F1 animals with the Neo cassette deleted. Reporter mice were housed in AAALAC-accredited animal facilities at the University of North Carolina, Chapel Hill (UNC) under specific-pathogen-free conditions. Protocols were approved by the UNC IACUC and complied with ethical regulations and humane endpoints.

In vivo mouse tumor studies. CT26 (ATCC, CRL-2638), 4T1 (ATCC, CRL-2539), B16-F0 (ATCC, CRL-6322), 3LL (ATCC, CRL-1642), and C1498 (TIB-49) were obtained from ATCC. After in vitro culture, cells were collected using TrypLE (Thermo Fisher), washed 3x in PBS, filtered through sterile 70 μ m strainer, then resuspended in PBS. Tumor cells were subcutaneously injected into the shaved right flank at the following specifications: 5×10^5 CT26 cells in 100 μ L PBS, 2×10^5 4T1 cells in 100 μ L PBS, 1×10^6 B16-F0 cells in 100 μ L PBS, and 1×10^6 3LL cells in 100 μ L PBS. C1498 cells were intravenously injected via lateral tail vein with 1×10^6 cells in 100 μ L PBS.

Murine Cytomegalovirus (MCMV) infection. Clinical condition and weights were recorded daily. Whole blood via tail vein bleed was obtained at designated time points. Mice were humanely euthanized at predetermined time points or earlier if $\geq 20\%$ weight loss was present or other pre-specified criteria were met.

Processing of mouse tissue. Mouse spleens were mechanically dissociated in PBS. Tissue was then strained through a 70 μ m filter and cells were treated with RBC lysis buffer for 5 minutes (BioLegend #420301). Cells were then washed with PBS, strained, and resuspended in PBS for analysis. Mouse livers were collected and mechanically dissociated in PBS.

Human clinical tumor and peripheral blood samples. Matched PBMCs from the same patients were isolated from whole blood by gradient centrifugation (Lymphocyte Separation Medium, Corning Life Sciences) followed by RBC lysis. Tumor samples

were obtained from fresh surgical specimens and placed into RPMI media. Single cell suspensions were generated from tumors by mechanical dissociation in PBS, filtered through 70 μm filters, incubated with RBC lysis buffer, and then resuspended at the desired concentration for flow cytometric analysis.

NK cells in vitro. Mouse, human, and canine NK cells were cultured in complete RPMI media (RPMI 1640 media (Invitrogen Life Technologies) supplemented with 10% Nu-Serum (Corning Life Sciences), 2mM L-glutamine (Glutamax®, Gibco), 1% non-essential amino acids (Gibco), $5 \times 10^{-5}\text{M}$ β -mercaptoethanol (MP Biomedicals), 1mM HEPES buffer (Corning Life Sciences), 1mM sodium pyruvate (Gibco), and 1% penicillin/streptomycin (Corning Life Sciences). For healthy human donors, as we had no access to information which could re-identify subjects, these samples were considered exempt from IRB approval.

RNA isolation, reverse transcription, and qRT-PCR. Fold expression was determined using the ΔCq method comparing gene of interest expression to housekeeper gene expression (GAPDH, B2M, IPO8). Relative fold expression was compared to unstimulated or untreated cells by the $2^{-\Delta\Delta\text{Cq}}$ method.